GPS Solutions (2022) 26:16
https://doi.org/10.1007/s10291-021-01201-3

GPS TOOLBOX

GIRAS: an open-source MATLAB-based software for GNSS-IR analysis

Cemali Altuntas[1] · **Nursu Tunalioglu**[1]

Received: 21 May 2021 / Accepted: 8 November 2021 / Published online: 25 November 2021

Abstract
Global Navigation Satellite System Interferometric Reflectometry (GNSS-IR) has become a robust method to extract the characteristic environmental features of reflected surfaces, where the signal transmitted from satellites reflects before receiving at GNSS antenna. When the signal arrives at the GNSS antenna from more than one path, a multipath error occurs, which causes interference of the direct and reflected signals. The interference of direct and reflected signals shows a pattern for sensing environmental features, where the signal reflects, and multipath directly affects the signal strength. Analyzing the signal strength represented by the signal-to-noise ratio (SNR) enables the retrieval of environment-related features. The software developed, named GIRAS (GNSS-IR Analysis Software), can process multi-constellation GNSS signal data and estimate the SNR metrics, namely phase, amplitude, and frequency, for further computations with several optional statistical analyses for controlling the quality of the estimations, as required, such as snow depth retrieval, effective reflector height estimation, and soil moisture monitoring. The software developed in the MATLAB environment has a graphical user interface. To represent the processes of the working procedures of the software, we conducted a case study with 7-day site data from the multi-GNSS experiment (MGEX) Project network displaying how to process GNSS data with input and output file properties.

Keywords GNSS-IR · SNR metrics · Statistical quality analysis · GIRAS

Introduction

The multipath effect in Global Navigation Satellite System (GNSS) technology is an undesired and dominant error source that should be eliminated for precise point positioning. However, GNSS interferometric reflectometry (GNSS-IR) has recently become a robust tool that uses the reflected signal quality to estimate the environment-related features of the reflected ground. If the satellite-emitted signal arrives at the GNSS antenna phase center (APC) following more than one path due to reflection surfaces surrounding the GNSS receiver location, reflected and direct signals are recorded simultaneously, which results in interference. A relative phase offset between direct and reflected signals occurs, resulting in an additional path that is proportional to the phase differences. The interference pattern of the direct and reflected signals shows a fluctuation/oscillation (Axelrad et al. 1996). The direct and reflected signal interference model is useful for extracting environmental parameters by analyzing the reflected GNSS signal phase, amplitude, and frequency. The signal-to-noise ratio (SNR) represents the strength of the signal recorded by GNSS receivers (Larson and Nievinski 2013) and the SNR observations recorded by GNSS receivers are used to estimate the signal quality and noise pattern of GNSS observations (Qian and Jin 2016).

The GNSS-IR technique implemented with a geodetic-grade GNSS antenna, which was designed to suppress the multipath effect, was first revealed by Larson et al. (2008a, b) for detecting soil moisture variations by SNR observables. Subsequently, the technique was successfully implemented

The GPS Tool Box is a column dedicated to highlighting algorithms and source code utilized by GPS engineers and scientists. If you have an interesting program or software package you would like to share with our readers, please pass it along; e-mail it to us at gpstoolbox@ngs.noaa.gov. To comment on any of the source code discussed here, or to download source code, visit our website at http://www.ngs.noaa.gov/gps-toolbox. This column is edited by Stephen Hilla, National Geodetic Survey, NOAA, Silver Spring, Maryland, and Mike Craymer, Geodetic Survey Division, Natural Resources Canada, Ottawa, Ontario, Canada.

✉ Cemali Altuntas
cemali@yildiz.edu.tr

1 Department of Geomatic Engineering, Yildiz Technical University, Istanbul, Turkey

for several environmental-related feature detection studies such as snow depth (Chen et al. 2014; Gutmann et al. 2012; Jin et al. 2016; Larson et al. 2009b; Ozeki and Heki 2012), vegetation models (Chew et al. 2016; Small et al. 2010; Wan et al. 2015), soil moisture (Altuntas and Tunalioglu, 2020; Han et al. 2020; Larson et al. 2008a,b, 2009a; Roussel et al. 2016; Zhang et al. 2017), landslide detection (Yang et al. 2019), and sea-level tides (Anderson 2000; Xi et al. 2018).

We introduce a new GUI-based software, GIRAS, that can process multi-constellation GNSS data and estimate SNR metrics, namely phase, amplitude, and frequency for feature extraction such as snow depth retrieval, effective reflector height estimation, and soil moisture monitoring. With a module included in the software, statistical analyses for controlling the quality and detecting the outliers of the estimations can be performed. Moreover, users can use the plot options to display the estimations and represent the sensed areas on the Google Earth map.

GNSS-IR and SNR Metrics

Bilich et al. (2007) described the relationship between the amplitudes and phases of direct and reflected signals through the phasor diagram when multipath was introduced. See Fig. 1. The carrier tracking loop shown in a phasor diagram with in-phase (I) and quadrature (Q) channels is shown in Fig. 1. The vector sum of the direct and reflected signals produces a composite signal, which is SNR observable.

From Bilich et al. (2007) and Larson and Nievinski (2013), the SNR data due to the direct signal plus one multipath reflection can be expressed in terms of amplitudes of the signals and phase by the following:

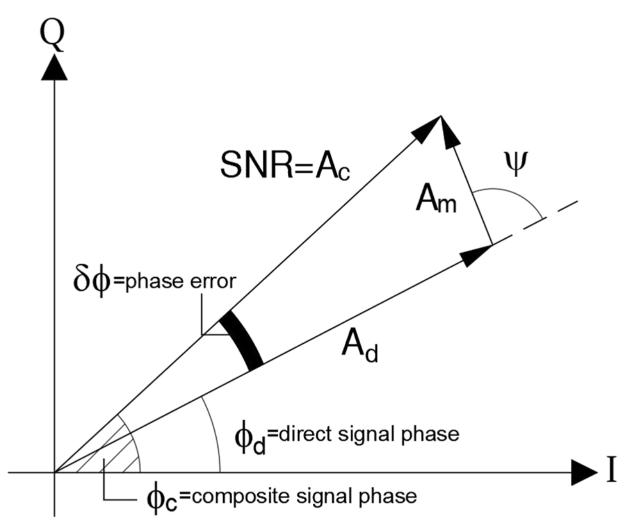

Fig. 1 Phasor diagram (following Bilich et al. 2007). I: In-phase component, Q: quadrature component

$$\mathrm{SNR}^2 \equiv A_c^2 = A_d^2 + A_m^2 + 2A_dA_m\cos\psi \quad (1)$$

Here the SNR is expressed as a function of the multipath amplitude A_m, direct amplitude A_d, and multipath relative phase ψ. Since GNSS satellites move continuously in the sky, changes in the geometry of reflection and thus ψ result in oscillations over the SNR (Larson et al. 2008a). The phase difference can be expressed as $\psi = (4\pi h/\lambda)\sin\varepsilon$, where λ is the GNSS wavelength, ε is the satellite elevation angle, and h is the vertical distance between the APC and ground.

As the composite signal includes the SNR data, the effect of direct and reflected signals should be separated to track the SNR variation due to multipath. Since $A_d \gg A_m$, the contribution of the direct signal over the trend of the composite signal can be eliminated by fitting a low-order polynomial. Then, the multipath pattern denoted as detrended SNR (dSNR) can be expressed as follows (Larson and Nievinski 2013):

$$\mathrm{dSNR} = A\cos\left(\frac{4\pi h}{\lambda}\sin\varepsilon + \phi\right) \quad (2)$$

where A and ϕ are the amplitude and phase offset of the reflected signal, respectively. Using the sine of the elevation angle as the independent variable, the oscillation frequency becomes a constant function of h. To estimate the SNR metrics, a Lomb–Scargle periodogram (LSP) can be implemented on the reflected signals for each satellite track (Hocke 1998; Lomb 1976; Scargle 1982). The outlier detection of the SNR metrics computed by LSP will be described in quality analysis of SNR metrics section.

The oscillations of the reflected signal are signs of fluctuations (Hefty and Gerhatova 2014), and the frequency of SNR oscillations is related to the effective reflector height between the APC and reflecting surface (Bilich and Larson 2007). The amplitude of SNR oscillations depends largely on surface reflectivity, and the phase offset directly relates to the apparent reflection depth of the GPS signal (Larson et al. 2008a). Once these SNR metrics, phase, amplitude, and frequency are estimated after analyzing the reflections of the GNSS signals, they can be used for environment-related retrieval facilities. Although the GNSS antenna records all available GNSS data transmitted from the satellites, the surrounding area where the receiver is located may not be suitable for retrieval studies. In some cases, the analysis of the SNR data recorded may be restricted by the surroundings, such as engineering structures, vegetation cover patterns, and forested areas from multiple directions. Thus, the sensed area should be mapped and represented. To overcome that, by selecting multiple azimuthal ranges from RINEX data, the first Fresnel zones (FFZs) should be drawn to show the GNSS footprints.

Quality analysis of SNR metrics

As is commonly known, errors in estimation raise uncertainty, which affects the reliability of the results. To eliminate this, outlier detection should be applied to the data. We added a series of options to obtain more stable results using criteria such as (1) limitations for minimum–maximum frequencies, (2) limitations for satellite elevation angles, (3) implementation of background noise condition (BNC), and (4) application of median absolute deviation (MAD) to the frequency, amplitude, or phase. The median method is implemented for the detection of outliers in SNR estimates as follows (Rousseeuw and Leroy 1987; Maronna et al. 2006; Hekimoglu et al. 2014):

$$med = median(\mathbf{s}), \tag{3}$$

$$MAD = 1.2533 \times \frac{1}{n} \times \sum |\mathbf{s} - med|, median|\mathbf{s} - med| = 0, \tag{4}$$

$$MAD = 11.4826 \times median|\mathbf{s} - med|, median|\mathbf{s} - med| \neq 0, \tag{5}$$

where $\mathbf{s}$ is the estimated SNR metric, *med* is the median value of the related estimation, and n is the length of the vector $\mathbf{s}$. In this method, the absolute median residuals ($|\mathbf{s} - med|$) are compared with the *MAD* values as a critical value. For the computation of *MAD* values, the median of median residuals is used. In some cases, the median of median residuals equals zero. In this case, Eq. 4 is used; otherwise, Eq. 5 is implemented. Here, if the median residuals are greater than the critical value, they are detected as outliers and removed from the estimations; otherwise, they are assigned as a good estimation and remain in the dataset.

GIRAS: GNSS-IR analysis software

GIRAS (GNSS-IR Analysis Software) is open-source software with file reading, data analysis, and data visualization tools. It was developed in MATLAB R2018b version. The software has a user-friendly interface with three main modules (tabs) and five submodules (subtabs). The software framework, including functions and modules, is given in Figs. 2 and 3 with brief explanations. In the data processing section, the codes of *get_ofac_hifac* and *lomb* are provided by Roesler and Larson (2018). Additionally, we used the codes of *refell* and *xyz2ell* in this software provided by Craymer (2021).

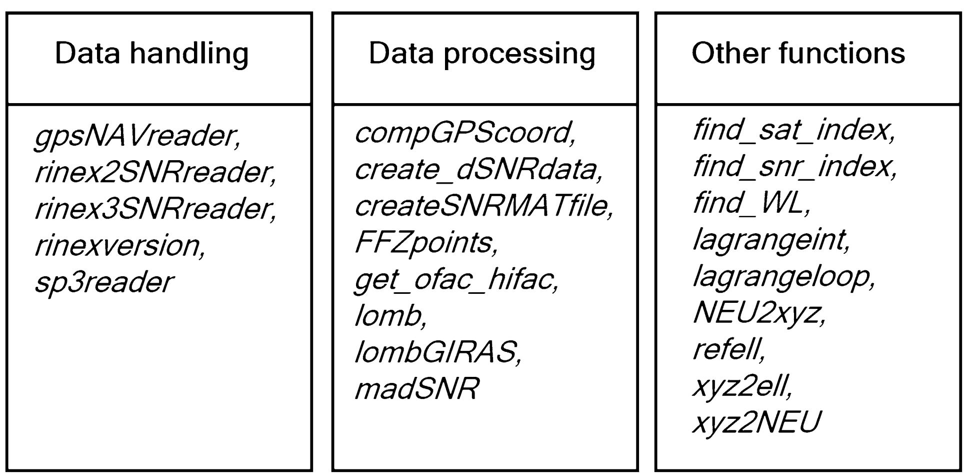

Fig. 2 Main functions of the GIRAS. Data handling functions are used to read raw data, data processing functions are used in pre-analysis and analysis modules, and other functions are the main supplementary function files

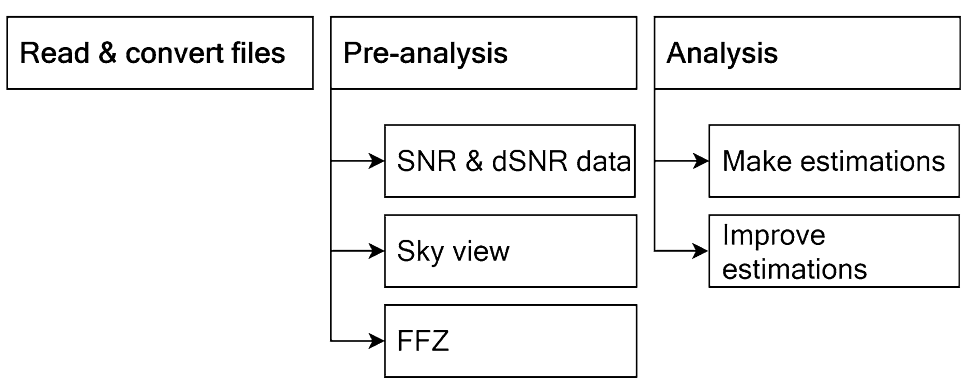

Fig. 3 Main modules and submodules of the GIRAS. Read & convert files: reading the raw GNSS data and preparing the necessary MAT files; pre-analysis: visualization and review of SNR & dSNR data and reflection zones; analysis: estimation of the SNR metrics and outlier analysis

Data handling

This module reads raw GNSS data and stores the necessary observations in the MATLAB environment. RINEX version 2 and RINEX version 3 observation files are supported. Both broadcast ephemeris (navigation file) and precise ephemeris (sp3) files can be used. While multi-GNSS (GPS, GLONASS, Galileo, Beidou) data are supported in precise ephemeris files, only GPS navigation files are supported as broadcast ephemeris. In addition, there is an input section for manually entering the receiver's position. In the user manual of GIRAS, the file capabilities for processes, inputs, outputs, and directories can be found.

Pre-analysis

This module enables reviewing the loaded and converted RINEX files in the first main module. It uses one of the SNRMAT files, which is one of the outputs of the first module. The first submodule of this module is called "SNR&dSNR data" and is used to plot SNR and dSNR data for each satellite and SNR observation type. Here, the user can select (1) data type: SNR or dSNR; (2) unit: dB or volts/volts; (3) time unit: hour or second; (4) angle limitations: azimuth and satellite elevation angle; (5) satellite track; and (6) polynomial degree. As different polynomial degrees are selected in this submodule, the plot screen on the side is updated instantly, thus allowing the user to visually select the most suitable trend. Here, the user can export the SNR & dSNR plot. In the second submodule, the sky view can be plotted as including the preferred satellite system/s. Sky plots can also be exported. In the third submodule, the FFZs in the study area can be plotted. The user can select the reflector height, satellite elevation angle, and SNR observation type as input; then, the FFZs can be displayed on the plot screen. In addition, the total number of satellite tracks, the distance between the ellipse center and the site, the area of an FFZ, and the total area of all FFZs are shown on the interface. The user can export the plot containing the FFZ areas as a MATLAB figure or a KML file that can be opened in Google Earth.

Analysis

The analysis module has two submodules. In the first submodule, "Make estimations," GNSS-IR metrics (frequency, amplitude, and phase) are estimated by using data from SNRMAT files, which is one of the outputs of the first module. The user can analyze one or more SNRMAT files here. There is a "settings" section in this submodule. Here, the user can set (1) the satellite systems to be used; (2) SNR observation type; (3) polynomial degree; (4) angle limitations: (a) a single range for the satellite elevation angle (b) one or more ranges for azimuth; (5) estimation options: (a) maximum reflector height (b) desired precision; and (6) name of the analysis results file. In the second submodule, "Improve estimations," the output of the first submodule is used as input. Then, four options are presented to the user to filter bad estimates in these data and improve the results. These are (1) minimum–maximum frequency; (2) minimum satellite elevation angle range; (3) BNC: 1 to 10 coefficient selection; and (4) MAD condition: selection of coefficients from 1 to 3 and selection of the metric based on which this condition will be applied (frequency, amplitude or phase). All available options for visualizing the results can be found in the user manual.

Finally, the output file provided by this submodule is saved in the "\results\best\" directory in both *.mat* and *.txt* formats. The structure of the output files (column numbers and descriptions) is given as follows: (1) Year, (2) DoY (day of year), (3) satellite PRN, (4) SNR type, (5) satellite track no, (6) satellite track type, (7) frequency, (8) amplitude, (9) phase, (10) first epoch, (11) last epoch, (12) number of epochs, (13) minimum elevation angle, (14) maximum elevation angle, (15) minimum azimuth angle, (16) maximum azimuth angle, (17) Max(P), and (18) background noise.

Case study example

To validate the GIRAS, an MGEX site, namely the Southern Great Plains Observatory (SGPO) (Fig. 4), which has multi-GNSS and multifrequency capability, was selected. The site information is given in Table 1.

The SGPO site data collected between January 1–7, 2021 (DoY 1–7), were analyzed. Precise ephemeris files provided by the Center for Orbit Determination in Europe (CODE) were used for satellite coordinates. The following are some of the outputs

Fig. 4 SGPO site—view from the northwest direction

Table 1 SGPO site info

Site name	Southern Great Plains Observatory
Four-character ID	SGPO
Country	United States of America (USA)
State	Oklahoma
Latitude	36.604°
Longitude	−97.485°
Height	290.200 m
GNSS receiver type	JAVAD TRE_3
GNSS antenna type	JAVRINGANT_G5T
Satellite systems	GPS + GLO + GAL + BDS
Elevation cutoff setting	0°
Data sampling interval	30 s
Date installed	1999-05-22

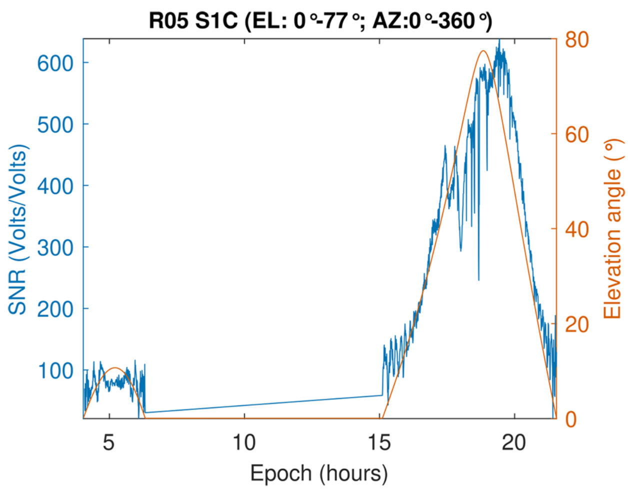

Fig. 5 R05 (GLONASS) S1C data and satellite elevation angles on January 01, 2021

provided by the software. S1C data and satellite elevation angles for the R05 satellite are shown in Fig. 5. In Fig. 6, the S1C data of the R05 satellite, SNR trend, and dSNR (0°–30° for satellite elevation angle range) are shown. A sky view of the SGPO site is given in Fig. 7. The FFZs for the 2-m reflector height and 5° satellite elevation angle are shown in Fig. 8.

The 7-day data from the SGPO site were analyzed by taking polynomial degree 2 with the 0°–30° satellite elevation angle limits and choosing the maximum reflector height of 5 m and the desired precision of 0.001 m, including all of the satellite systems and observation types. Considering 7 days of observations, the total number of estimates and their distribution according to the satellite system and observation type are given in Table 2.

Since different types of observations have different frequencies, only one frequency should be selected when

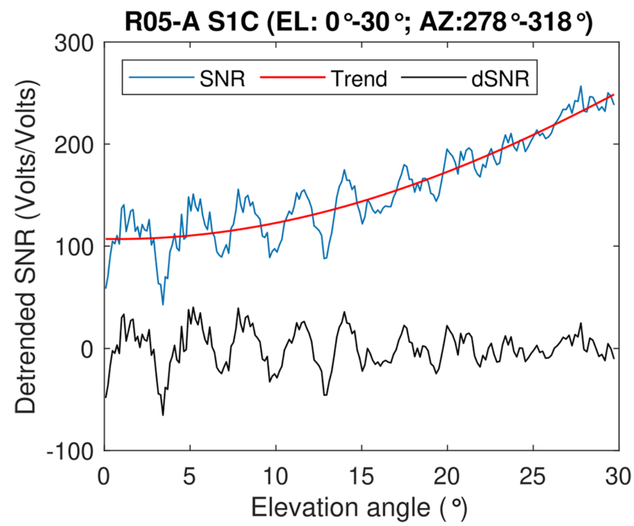

Fig. 6 R05 (GLONASS) S1C data, SNR trend and dSNR for the 0°–30° satellite elevation angle range on January 01, 2021. A second-order polynomial was implemented to obtain the trend indicated with the red line

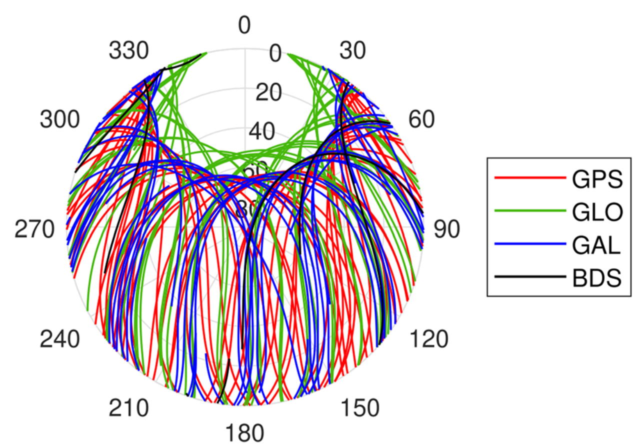

Fig. 7 Sky view of SGPO site on January 01, 2021

performing a frequency-based outlier analysis. In this example, the S1C data with the most estimates were evaluated. In Fig. 9 (left panels), the results are represented without implementing any outlier analysis option. The estimates remaining after outlier analysis are shown in the right panels. As can be seen, the outlier analysis significantly improved the results.

Conclusion

As the SNR data recorded at the GNSS antenna are an indicator of the signal strength, the SNR metrics estimated by analyzing the interference pattern are useful parameters for environmental sensing. This study represents software

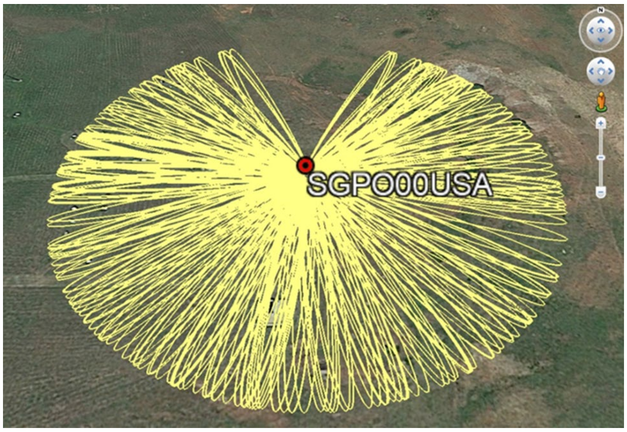

Fig. 8 FFZs for 2-m reflector height and 5° satellite elevation angle on January 01, 2021

Table 2 Number of estimates with satellite systems

	Satellite system				
	GPS	GLO	GAL	BDS	ALL
SNR type					
S1C	734	583	–	–	1317
S1P	–	581	–	–	581
S1W	729	–	–	–	729
S1X	–	–	481	–	481
S2C	–	584	–	–	584
S2I	–	–	–	67	67
S2P	–	571	–	–	571
S2W	729	–	–	–	729
S2X	532	–	–	–	532
S3X	–	55	–	–	55
S5X	373	–	481	–	854
S6I	–	–	–	81	81
S6X	–	–	481	–	481
S7I	–	–	–	81	81
S7X	–	–	481	–	481
S8X	–	–	481	–	481
ALL	3097	2374	2405	229	8105

developed to estimate the amplitude and phase of reflected signals and subsequently compute reflector height. The software with modules enables the selection of azimuthal and elevation angle masks with multiple range selections for either short-term or long-term GNSS data collected, which may help to predict future models for climatological studies. The software is also suitable for multi-GNSS analysis in which the desired system(s) can be selected for analysis. The quality-control modules are multiple-choice modules. The output files are well designed for users in a defined format for further computations.

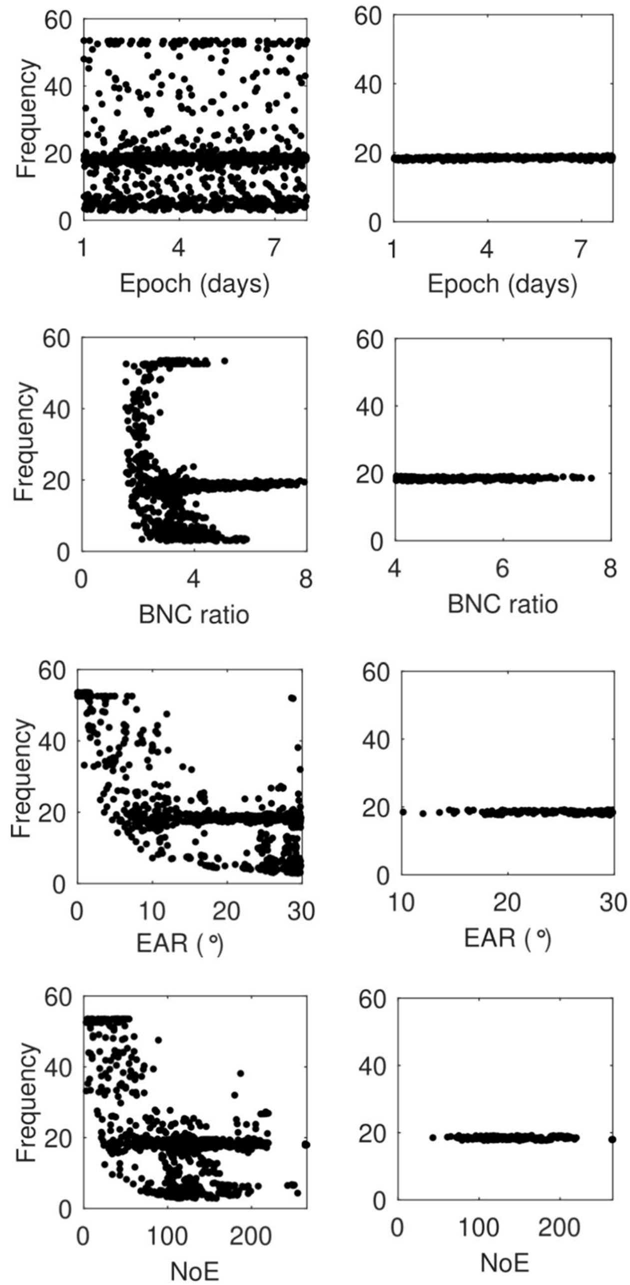

Fig. 9 Plot examples of results obtained from the analysis of 7-day (January 01–07, 2021) S1C data. EAR: Elevation angle range, NoE: number of epochs. The minimum EAR was set at 10°, the BNC at 4, and the MAD at 1. All results (left column); results after outlier analysis (right column)

Acknowledgements We would like to thank The Crustal Dynamics Data Information System (CDDIS) and the Center for Orbit Determination in Europe (CODE) for the GNSS data and IGS precise orbits and open-access MATLAB codes provided by Roesler and Larson (2018) and Craymer (2021).

Data availability The MATLAB source code, sample data, and user manual for the software are available on the GPS Toolbox website at https://geodesy.noaa.gov/gps-toolbox.

References

Altuntas C, Tunalioglu N (2020) Estimation performance of soil moisture with GPS-IR method. Sigma: J Eng Nat Sci 38(4):2217-2230

Anderson KD (2000) Determination of water level and tides using interferometric observations of GPS signals. J Atmos Oceanic Tech 17(8):1118–1127. https://doi.org/10.1175/1520-0426(2000)017%3c1118:DOWLAT%3e2.0.CO;2

Axelrad P, Comp CJ, MacDoran PF (1996) SNR-based multipath error correction for GPS differential phase. IEEE Trans Aerosp Electron Syst 32(2):650–660

Bilich A, Axelrad P, Larson KM (2007) Scientific utility of the signal-to-noise ratio (SNR) Reported by Geodetic GPS Receivers, Proc. ION GNSS 2007, Institute of Navigation, Nashville, Tennessee, USA, September 25–28, 1999–2010.

Bilich A, Larson KM (2007) Mapping the GPS multipath environment using the signal-to-noise ratio (SNR). Radio Sci. https://doi.org/10.1029/2007RS003652

Chen Q, Won D (2014) Akos DM (2014) Snow depth sensing using the GPS L2C signal with a dipole antenna. EURASIP J Adv Signal Process 1:106. https://doi.org/10.1186/1687-6180-2014-106

Chew C, Small EE, Larson KM (2016) An algorithm for soil moisture estimation using GPS-interferometric reflectometry for bare and vegetated soil. GPS Sol 20(3):525–537. https://doi.org/10.1007/s10291-015-0462-4

Craymer M (2021) Geodetic Toolbox. MATLAB central file exchange (https://mathworks.com/matlabcentral/fileexchange/15285-geodetic-toolbox).

Gutmann ED, Larson KM, Williams MW, Nievinski FG, Zavorotny V (2012) Snow measurement by GPS interferometric reflectometry: an evaluation at Niwot Ridge. Colorado Hydrol Process 26(19):2951–2961. https://doi.org/10.1002/hyp.8329

Han M, Zhu Y, Yang D, Chang Q, Hong X, Song S (2020) Soil moisture monitoring using GNSS interference signal: proposing a signal reconstruction method. Remote Sens Lett 11(4):373–382. https://doi.org/10.1080/2150704X.2020.1718235

Hefty J, Gerhatova LU (2014) Using GPS multipath for snow depth sensing-first experience with data from permanent stations in Slovakia. Acta Geodyn Geomater 11(1):53–63. https://doi.org/10.13168/AGG.2013.0055

Hekimoglu S, Erdogan B, Soycan M, Durdag UM (2014) Univariate approach for detecting outliers in geodetic networks. J Surv Eng 140(2):04014006. https://doi.org/10.1061/(ASCE)SU.1943-5428.0000123

Hocke K (1998) Phase estimation with the Lomb-Scargle periodogram method. Ann Geophys-Eur Geophys Soc 16:356–358

Jin S, Qian X, Kutoglu H (2016) Snow depth variations estimated from GPS-Reflectometry: a case study in Alaska from L2P SNR data. Remote Sensing 8(1):63. https://doi.org/10.3390/rs8010063

Larson KM, Braun JJ, Small EE, Zavorotny VU, Gutmann ED, Bilich AL (2009a) GPS multipath and its relation to near-surface soil moisture content. IEEE J Select Topics Appl Earth Observ Remote Sens 3(1):91–99. https://doi.org/10.1109/JSTARS.2009.2033612

Larson KM, Gutmann ED, Zavorotny VU, Braun JJ, Williams MW, Nievinski FG (2009) Can we measure snow depth with GPS receivers? Geophys Res Lett. https://doi.org/10.1029/2009GL039430

Larson KM, Nievinski FG (2013) GPS snow sensing: results from the EarthScope Plate Boundary Observatory. GPS Solutions 17(1):41–52. https://doi.org/10.1007/s10291-012-0259-7

Larson KM, Small EE, Gutmann ED, Bilich AL, Axelrad A, Braun JJ (2008) Using GPS multipath to measure soil moisture fluctuations: initial results. GPS Sol 12(3):173–177

Larson KM, Small EE, Gutmann ED, Bilich AL, Braun JJ, Zavorotny VU (2008) Use of GPS receivers as a soil moisture network for water cycle studies. Geophys Res Lett 35:L24405

Lomb NR (1976) Least-squares frequency analysis of unequally spaced data. Astrophys Space Sci 39(2):447–462

Maronna RA, Martin DR, Yohai VJ (2006) Robust statistics: theory and methods. Wiley Series in Probability and Statistics, New York

Masters D, Axelrad P, Katzberg S (2004) Initial results of land-reflected GPS bistatic radar measurements in SMEX02. Remote Sens Environ 92(4):507–520. https://doi.org/10.1016/j.rse.2004.05.016

Ozeki M, Heki K (2012) GPS snow depth meter with geometry-free linear combinations of carrier phases. J Geodesy 86(3):209–219. https://doi.org/10.1007/s00190-011-0511-x

Qian X, Jin S (2016) Estimation of snow depth from GLONASS SNR and phase-based multipath reflectometry. IEEE J Select Topics Appl Earth Observ Remote Sens 9(10):4817–4823. https://doi.org/10.1109/JSTARS.2016.2560763

Roesler C, Larson KM (2018) Software tools for GNSS interferometric reflectometry (GNSS-IR). GPS Solut 22(3):80

Rousseeuw PJ, Leroy AM (1987) Robust regression and outlier detection, vol 1. Wiley, New York

Roussel N, Frappart F, Ramillien G, Darrozes J, Baup F, Lestarquit L, Ha MC (2016) Detection of soil moisture variations using GPS and GLONASS SNR data for elevation angles ranging from 2 to 70. IEEE J Select Topics Appl Earth Observ Remote Sens 9(10):4781–4794. https://doi.org/10.1109/JSTARS.2016.2537847

Scargle JD (1982) Studies in astronomical time series analysis. II-Statistical aspects of spectral analysis of unevenly spaced data. Astrophys J 263:835–853

Small EE, Larson KM, Braun JJ (2010) Sensing vegetation growth with reflected GPS signals. Geophys Res Lett 37(12):L12401. https://doi.org/10.1029/2010GL042951

Wan W, Larson KM, Small EE, Chew CC, Braun JJ (2015) Using geodetic GPS receivers to measure vegetation water content. GPS Sol 19:237–248. https://doi.org/10.1007/s10291-014-0383-7

Xi R, Zhou X, Jiang W, Chen Q (2018) Simultaneous estimation of dam displacements and reservoir level variation from GPS measurements. Measurement 122:247–256. https://doi.org/10.1016/j.measurement.2018.03.036

Yang Y, Zheng Y, Yu W, Chen W, Weng D (2019) Deformation monitoring using GNSS-R technology. Adv Space Res 63(2019):3303–3314

Zhang S, Roussel N, Boniface K, Ha MC, Frappart F, Darrozes J, Baup F, Calvet JC (2017) Use of reflected GNSS SNR data to retrieve either soil moisture or vegetation height from a wheat crop. Hydrol Earth Syst Sci 21:4767–4784. https://doi.org/10.5194/hess-21-4767-2017

Cemali Altuntas received the B.Sc. and M.Sc. degrees in geomatics from Yildiz Technical University, Istanbul, Turkey. He works as a research assistant in the Department of Geomatic Engineering at the same university. His research is mainly focused on GNSS Interferometric Reflectometry (GNSS-IR) and its implementation.

Nursu Tunalioglu received her Ph.D. degree in geomatic engineering from Yildiz Technical University, Istanbul, Turkey, in 2011. She is currently working as an associate professor at the same university. Her research interests include engineering surveys, highway planning, GNSS and high-accurate GNSS positioning, and GNSS-IR.